Journal of Materials and Engineering

Corrosion Inhibition of Mild Steel in HCl Solution Using MPO: Experimental and Theoretical Insights

Iman Adnan Annon[a] , Khaldoon K. Jlood[a], Mahdi M. Hanoon[a] , Firas F. Sayyid[a] ,
Waleed K. Al-Azzawi[b] , Ahmed Al-Amiery[c],*

[a]Production and Metallurgy Engineering Department, University of Technology, 10001, Baghdad, Iraq,
[b]Al-Farahidi University, 10001, Baghdad, Iraq,
[c]Department of Chemical and Process Engineering, Faculty of Engineering and Built Environment, Universiti Kebangsaan Malaysia, Bangi, Malaysia.
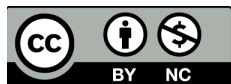
A B S T R A C T

Corrosion is a pervasive challenge in various industrial applications, particularly in acidic environments. This comprehensive study delves into the effectiveness of 2-methyl-4-propyl-1,3-oxathiane (MPO) as a corrosion inhibitor for mild steel exposed to hydrochloric acid (HCl) solutions. The investigation employs weight loss techniques to assess the inhibitor's performance over varying durations (ranging from 1 to 48 hours) and concentrations (0.1 to 1 mM). At a concentration of 0.5 mM, the inhibitor demonstrates impressive inhibitory efficiency, ranging from 87.6% at 303 K to 92.9% at 333 K during a 5-hour exposure period. Additionally, the impact of temperature on the corrosion inhibition process is examined at temperatures of 303, 313, 323, and 333 K, showing substantial inhibition efficiencies. Quantum chemical calculations using Density Functional Theory (DFT) methods elucidate the molecular interactions between MPO and the metal surface. Notably, the analysis of EHOMO (Highest Occupied Molecular Orbital Energy), ELUMO (Lowest Unoccupied Molecular Orbital Energy), Egap (Energy Gap), total hardness (η), electronegativity (χ), and electron fraction transition atom (ΔN) reveals valuable insights into MPO's corrosion inhibition capabilities. The outcomes underscore MPO's potential as an effective corrosion inhibitor for mild steel in HCl environments, laying the groundwork for more efficient corrosion prevention strategies in industrial settings.

1. INTRODUCTION

Corrosion is a pervasive and costly issue that affects various industries, including manufacturing, infrastructure, and transportation.

The gradual deterioration of metallic materials due to chemical reactions with their surrounding environment can lead to significant economic losses and safety hazards. In particular, mild steel, a commonly used

construction material, is susceptible to corrosion, making it essential to develop effective corrosion inhibition strategies [1-5]. Corrosion inhibition is a vital aspect of materials science and engineering aimed at mitigating the adverse effects of corrosion. By introducing corrosion inhibitors, we can protect metallic structures and extend their service life, reducing maintenance costs and minimizing environmental impacts. This study focuses on the potential of MPO as a corrosion inhibitor for mild steel, exploring its inhibitory properties in acidic environments [6-10]. Acidic environments, such as hydrochloric acid (HCl) solutions, are known to be highly corrosive to metals. Understanding and controlling corrosion in such environments is of paramount importance due to their widespread industrial use and potential for causing severe damage [11-15]. This research investigates the corrosion inhibition capabilities of MPO specifically in HCl solutions. The primary purpose of this study is to assess the effectiveness of MPO (Figure 1) as a corrosion inhibitor for mild steel in HCl solution.
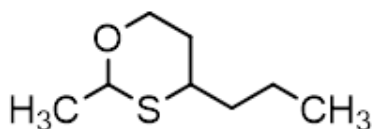
Fig. 1. The chemical structure of MPO.

By conducting a comprehensive investigation, we aim to provide insights into its corrosion inhibition performance under varying conditions, including inhibitor concentrations, exposure durations, and temperatures.

The research objectives of this study can be summarized as follows:

1. Evaluate the corrosion inhibition efficiency of MPO for mild steel in HCl solution.

2. Investigate the influence of inhibitor concentration on corrosion inhibition.

3. Examine the effect of exposure duration on corrosion inhibition.

4. Assess the impact of temperature on the corrosion inhibition process.

5. Perform quantum chemical calculations to elucidate the molecular interactions between the inhibitor and the metal surface.

To achieve the research objectives, a combination of experimental and computational approaches will be employed. The experimental aspect involves the use of weight loss techniques to measure corrosion rates over different time periods and inhibitor concentrations. The computational aspect utilizes Density Functional Theory (DFT) methods to calculate quantum parameters and gain insights into the inhibitor's chemical behavior and its interaction with mild steel.

2. LITERATURE REVIEW

Corrosion of mild steel is a complex electrochemical process influenced by various factors, including the presence of corrosive agents, such as acids. In acidic environments, corrosion typically involves the dissolution of iron (Fe) and the formation of iron ions (Fe^{2+}) along with the release of hydrogen gas (H_2). The process is influenced by factors like pH, temperature, and the concentration of corrosive species. Understanding the fundamental corrosion mechanisms in mild steel provides the basis for developing effective corrosion inhibition strategies [16-20]. Corrosion inhibition methods aim to mitigate the destructive effects of corrosion by introducing chemical compounds known as inhibitors. These inhibitors form protective layers on the metal surface, reducing the rate of corrosion. Various types of inhibitors, including organic compounds, inorganic compounds, and mixed inhibitors, have been explored. In particular, organic corrosion inhibitors have gained attention for their ability to form stable adsorption layers on metal surfaces, hindering the corrosion process. This study focuses on MPO as a potential organic inhibitor for mild steel in acidic environments [21-25]. Prior research efforts have explored the use of different corrosion inhibitors for mild steel in acidic solutions. These studies have investigated the inhibition efficiency of various organic compounds, such as amines, thioureas, and thiazoles. While some inhibitors have shown promise, their effectiveness can vary significantly depending on factors like concentration, exposure duration, and temperature. A comprehensive review of previous studies provides valuable insights into the performance of corrosion inhibitors and informs the design of new inhibitor formulations [26-30]. Quantum chemical calculations, particularly using Density

Functional Theory (DFT) methods, have emerged as powerful tools for understanding the molecular-level interactions between inhibitors and metal surfaces. These calculations provide insights into key parameters such as $E_{(HOMO)}$ (Highest Occupied Molecular Orbital Energy), $E_{(LUMO)}$ (Lowest Unoccupied Molecular Orbital Energy), and the Energy Gap (E_{gap}). Additionally, quantum parameters such as total hardness (η), electronegativity (χ), and electron fraction transition atom (ΔN) play crucial roles in elucidating the inhibitory behavior of compounds [31-35]. The significance of quantum chemical calculations in corrosion inhibition lies in their ability to predict inhibitor effectiveness, understand adsorption mechanisms, and guide the design of novel inhibitors with enhanced properties. By bridging the gap between theory and experiment, these calculations contribute to the development of more efficient corrosion prevention strategies [36-39].

3. EXPERIMENTAL

3.1 Materials

Reagent-grade chemicals obtained from Sigma-Aldrich in KL, Malaysia, were used without further purification. The mild steel samples were procured from Metal Samples Company and had the following elemental composition by weight percentage: Carbon, 21×10^{-2}; Manganese, 5×10^{-2}; Silicone, 38×10^{-2}; Aluminum, 10^{-2}; Sulfur, 5×10^{-2}; Phosphorous, 9×10^{-2}; with Iron as the remainder. For weight loss measurements, coupons with dimensions measuring $4.0 \times 2.5 \times 0.1$ cm were used. These coupons were initially treated by grinding with emery paper, starting with grade 400, followed by 600, and finally 1200. Subsequently, they were thoroughly cleansed with double-distilled water to remove any residual particles, followed by a degreasing step using ethanol. Afterward, the coupons were allowed to air dry at room temperature.

3.2 Test Solutions

A 1M hydrochloric acid (HCl) solution was prepared by diluting 37% analytical grade HCl from Malaysia with double-distilled water. The inhibitor's concentration was adjusted by adding varying amounts of the tested inhibitor to the hydrochloric acid, followed by thorough mixing to ensure a homogeneous solution. To evaluate the solution's corrosiveness, metallic samples were immersed in it for a specified duration. Subsequent visual inspections of the samples were conducted to detect any changes in appearance, such as pitting, discoloration, or loss of thickness. Additionally, the mass of the coupons was measured to quantify the extent of corrosion. The effectiveness of the inhibitor in mitigating corrosion in corrosive media was determined based on the outcomes of these evaluations.

3.3 Weight loss Techniques

The gravimetric approach, recommended by the National Association of Corrosion Engineers (NACE), was used to determine the corrosion rate (CR), inhibitive performance (IE%), and surface coverage (θ). Metallic samples were immersed in a 1M HCl solution for 5 hours. During this immersion, varying concentrations of the inhibitor (ranging from 0.1 to 0.5 mM) were introduced to act as a corrosion inhibitor. This process was carried out at different temperatures, ranging from 303 to 333 K. To investigate the influence of immersion duration, metal samples were exposed to the 1M HCl solution at a constant temperature of 303 K. However, for varying immersion durations (1, 5, 10, 24, and 48 hours), the same procedure was followed. In this case as well, various concentrations of the inhibitor (ranging from 0.1 to 0.5 mM) were introduced as a corrosion inhibitor [40,41].

To calculate the corrosion rate, inhibition efficiency, and surface coverage, the following equations were employed:

Corrosion Rate (C_R (mm/y)):

$$C_R = \frac{\Delta W}{At}$$

Where:

ΔW is the weight loss of the sample.

A is the exposed surface area of the sample.

t is the exposure duration.

Inhibition Efficiency (IE%):

$$IE\% = \frac{C_{R0} - C_{Ri}}{C_{R0}} \times 100$$

Where:

C_{R0} is the corrosion rate of the uninhibited solution.

C_{Ri} is the corrosion rate with the inhibitor.

Surface Coverage (θ):

$$\theta = \frac{C_{R0} - C_{Ri}}{C_{R0}}$$

3.4 Adsorption Isotherms

The adsorption isotherm type is a valuable tool for understanding the interaction between the inhibitor and the metal surface. To determine these isotherms, it is crucial to calculate the surface coverage degree (θ) of the tested inhibitor. This calculation involves fitting experimental data to various adsorption models, including, but not limited to, the Langmuir, Frumkin, and Temkin models. Herein, we obtained θ values through the application of the following equations [42]:

Langmuir equation: $\theta = K \times C1 + K \times C$

Frumkin equation: $\theta = K \times C1 + K \times C + K2 \times C2$

Temkin equation: $\theta = K \times (1 + K \times C)2$

Here, θ signifies the surface coverage, K represents the equilibrium constant, and C stands for the concentration of the inhibitor.

3.5. Computational Investigations

We utilized Gaussian 09 software for our quantum calculations. The optimization of the inhibitor's structure in a gaseous phase was conducted using the B3LYP method with a 6–31G++(d,p) basis set. To determine the ionization potential (I) and electron affinity (A), denoted as EHOMO and ELUMO, respectively, we employed Koopman's theorem [43]. These values were derived via the following equations:

Ionization Potential (I) or EHOMO: $I = -EHOMO$

Electron Affinity (A) or ELUMO: $A = -ELUMO$

Additionally, we calculated several other parameters, including hardness (η), electronegativity (χ), softness (σ), and the fractional number of transferred electrons (ΔN), using the following relationships:

Hardness (η): $\eta = 12(I - A)$

Electronegativity (χ): $\chi = 12(I + A)$

Softness (σ): $\sigma = 1/\eta$

Number of Transferred Electrons (ΔN): $\Delta N = 7 - \chi inh / 2 \eta inh$

These equations are used to determine the fractional number of electrons transferred during a chemical reaction or adsorption process, taking into account the electronegativity and hardness of the involved species, whether it be the inhibitor or the metal (iron, in this case). These computational investigations yielded crucial insights into the electronic and chemical attributes of the inhibitor, facilitating a deeper comprehension of its molecular-level behavior and interactions

4. RESULTS AND DISCUSSION

4.1 Weight Loss Tests

The evaluation of corrosion inhibition efficiency is a pivotal aspect of our study, as it provides insights into the effectiveness of the MPO inhibitor in mitigating corrosion in HCl solution. Several key factors, including concentration, temperature, and exposure time, were systematically examined to assess the inhibitor's performance.

4.1.1 Effect of Concentration

The impact of inhibitor concentration on corrosion inhibition was investigated at a temperature of 303 K during a 5-hour exposure period. Increasing the concentration of the inhibitor resulted in enhanced corrosion inhibition capability. Specifically, as the concentration of the inhibitor increased, the corrosion rate decreased. The highest inhibitory efficiency, reaching 87.6%, was achieved at a concentration of 0.5 mM. This improved protective effect can be attributed to the presence of the thioxane ring in the inhibitor, which elevates the electron density at active sites (Figure 2).
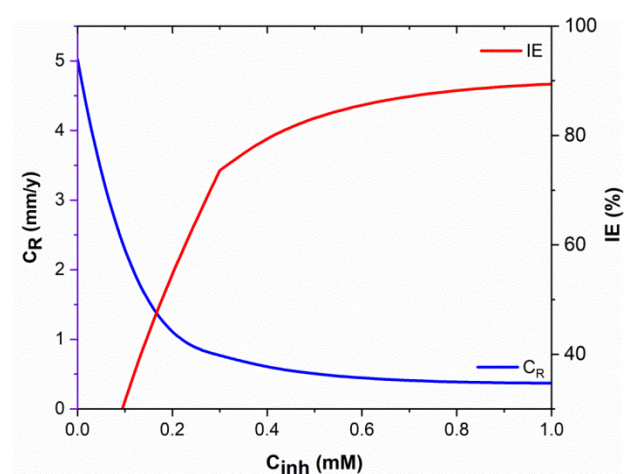

**Fig. 2**. Effect of inhibitor concentration.

This, in turn, enables more effective interactions with iron atoms, as well as oxygen and sulfide atoms on the metal surface, contributing to its inhibitory prowess by forming coordination bonds with the metal. These interactions enhance the inhibitor's ability to inhibit corrosion. It's important to recognize that the impact of different inhibitor concentrations in a 1M HCl solution can vary, and finding the optimal concentration may depend on factors such as the particular inhibitor, temperature, and the presence of other substances [44,45].

The inhibitory efficiency of thioxane derivative molecules against acidic corrosion remains effective up to a concentration of 0.5 mM. This effectiveness arises from the adsorption of these molecules onto the tested coupon surfaces, forming a protective film. Within the concentration range of 0.5–1.0 mM, inhibitory efficiency retains a high level, creating a barrier effect against corrosive agents and further reducing the corrosion rate. The protective film can also absorb corrosive species and neutralize them, contributing to the overall reduction in the corrosion rate. The presence of thioxane derivative molecules in the protective film further decelerates the corrosion rate by forming robust bonds, creating a dense and stable layer that acts as a barrier against corrosion. Numerous studies have explored the effects of different inhibitor concentrations on mild steel corrosion rates in acidic solutions, and this study aligns with those findings, demonstrating the concentration-dependent behavior of inhibitors [46,47].

4.1.2 Effect of Temperature

To investigate the influence of temperature on the corrosion inhibition properties, we conducted tests following a 5-hour immersion period at a range of temperatures from 303 to 333 K. The results at a concentration of 0.5 mM were particularly noteworthy. Based on Figure 3, at lower temperatures, such as 303 K, the inhibitor exhibited a substantial inhibition efficiency, registering at 87.6%. As the temperature increased to 313 K, 323 K, and 333 K, the inhibition efficiencies continued to rise, measuring at 89.1%, 91.8%, and 92.9%, respectively. Similarly, when the inhibitor concentration was increased to 1.0 mM, the inhibition efficiencies also showed an upward trend: 89.4% at 303 K, 90.1% at 313 K,

92.8% at 323 K, and an impressive 95.6% at 333 K. This intriguing rise in inhibition efficiency with increasing temperature can be attributed to a combination of chemisorption and physisorption mechanisms. At higher temperatures, the kinetic energy of molecules in the solution increases, promoting more frequent collisions between the inhibitor and the mild steel surface [48,49]. These collisions lead to stronger adsorption of the inhibitor molecules onto the metal surface. Furthermore, the enhanced inhibition at elevated temperatures can be explained by considering the energetics of adsorption. At higher temperatures, the activation energy required for the inhibitor molecules to chemisorb onto the metal surface is more readily overcome. This facilitates stronger chemical bonding between the inhibitor and the iron atoms on the mild steel surface, resulting in improved corrosion inhibition. Moreover, the physisorption mechanism, which involves weaker interactions between the inhibitor and the metal surface, becomes more favorable at higher temperatures due to increased thermal motion of the inhibitor molecules. This means that the inhibitor molecules can attach to the metal surface more easily through physical adsorption, in addition to the enhanced chemical bonding [50,51].
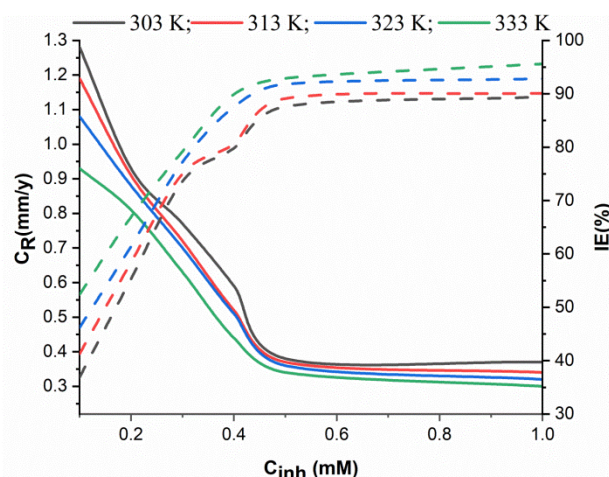
Fig. 3. Effect of Temperature.

In summary, the observed increase in inhibition efficiency with rising temperature can be attributed to the combined effects of increased collision frequency, lowered activation energy for chemisorption, and enhanced physisorption at higher temperatures. These factors contribute to the inhibitor's heightened performance in mitigating corrosion as the temperature of the environment increases.

4.1.3 Effect of Time

The effect of time on corrosion inhibition was examined at 303 K. The findings regarding Figure 4, revealed that longer immersion periods led to more substantial corrosion reduction. For instance, the lowest corrosion rate was recorded after a 24-hour immersion at a concentration of 1.0 mM, revealing a 77% reduction compared to a 1-hour immersion period. These results suggest that the inhibitor might present a viable alternative to conventional corrosion inhibitors. The inhibitory effectiveness increased rapidly within the initial 10 hours of immersion, remained relatively stable during the subsequent 10–24 hours, and gradually declined beyond the 24-hour mark [52,53]. Extended immersion periods resulted in a higher concentration of inhibitor molecules forming a consistent coating that hindered the corrosion process. However, as the immersion period exceeded 24 hours, the inhibitor's effectiveness decreased. The efficacy of inhibition is also contingent on other factors, including pH, temperature, and the concentration of the inhibitor solution. In summary, the inhibitory efficacy of the inhibitor depends on numerous factors, including immersion duration. The most substantial inhibitory efficacy is typically observed during immersion periods spanning from 10 to 24 hours. The reasonably high inhibitory efficacy during prolonged exposure suggests that the inhibitor layer adsorbed on the metal surface obstructs the ingress of corrosive agents, contributing to its stability and effectiveness as a corrosion inhibitor in acidic environments [54,55].
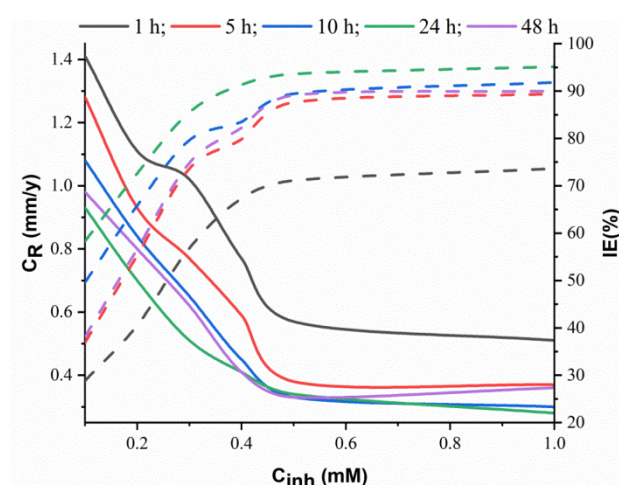

Fig. 4. Effect of immersion time.

4.2 Adsorption isotherm

Understanding the adsorption of inhibitor molecules onto the metallic substrate is crucial in elucidating the corrosion inhibition process. To gain insights into this phenomenon, we conducted gravimetric assessments to determine the surface coverage (θ) values of the inhibitor. Subsequently, we applied the Temkin, Freundlich, and Langmuir isotherm models to investigate the adsorption mechanism. The Langmuir isotherm model emerged as the most suitable description of the adsorption process. This model suggests that adsorption takes place in a monolayer manner, with metal ions adhering to the adsorbent's surface at a fixed maximum capacity. In contrast, the Temkin isotherm model indicated that the adsorption process is primarily driven by the heat of adsorption, implying that metal ions attach to the adsorbent's surface through physisorption. On the other hand, the Freundlich isotherm model hinted that adsorption is influenced by the heterogeneity of the adsorbent's surface, implying a multilayer adsorption process. These findings collectively indicate that the adsorption of metal ions onto the adsorbent involves a combination of physisorption and chemisorption, with physisorption being the dominant mechanism. The Langmuir isotherm model played a crucial role in determining the maximum capacity of the adsorbent and the uptake of metal ions under various conditions. Conversely, the Temkin and Freundlich isotherms provided valuable insights into the nature of the adsorption process and the roles of heat and surface heterogeneity, respectively [56,57]. These revelations have practical significance for the development and optimization of adsorption processes aimed at removing metal ions from aqueous solutions. Moreover, the Langmuir adsorption isotherms closely align with the experimental data, as indicated by the intercepts, slopes, and high regression coefficients (R^2) obtained at different temperatures (303 K, 313 K, 323 K, and 333 K). Figure 5 illustrates the Langmuir adsorption isotherm plot between C_inh/θ and C_inh, with adsorption parameters determinable through the following equation:

$$C_{inh}/\theta = (K_{ads})^{-1} + C_{inh}$$

where C_inh is the inhibitor concentration, θ is the surface area, and K_ads is the constant of the equilibrium.

The adsorption parameters ΔG^o_{ads} and K_{ads} were determined by plotting C/ θ against C, using the below equation for the calculations.

$$\Delta G^o_{ads} = -RT\ ln(55.5\ K_{ads})$$

The value 55.5 represents the molar concentration of water, while R denotes the universal gas constant and T indicates the absolute temperature.
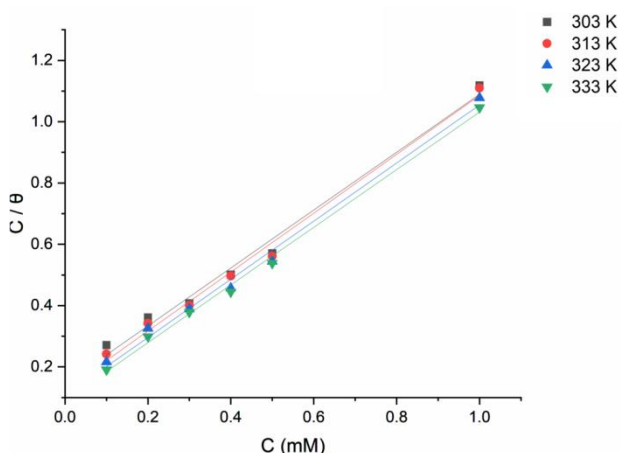
Fig. 5. Langmuir adsorption isotherm plot.

The value of ΔG^o_{ads} plays a crucial role in deciphering the nature of the adsorption process. Generally, when ΔG^o_{ads} is in the vicinity of and more negative than $-40\ kJmol^{-1}$ it typically signifies a chemisorption mechanism, which involves the formation of strong and stable chemical bonds between the adsorbate (inhibitor) and the adsorbent (metal surface). Conversely, when ΔG^o_{ads} approaches and is less negative than $-40\ kJmol^{-1}$, it suggests a physisorption mechanism. Physisorption involves weaker physical interactions, such as van der Waals forces, between the adsorbate and adsorbent. In the context of our inhibitor, the ΔG^o_{ads} value falls within the range of $-20\ kJmol^{-1}$ to $-40\ kJmol^{-1}$. This range indicates a coexistence of both chemisorption and physisorption mechanisms. The negative sign of ΔG^o_{ads} indicates the spontaneity of the adsorption process, implying that adsorption is a favorable and energetically feasible process [58,59]. The magnitude of ΔG^o_{ads}, which is moderately negative, suggests that chemisorption takes precedence in the adsorption process. This is indicative of a stable and irreversible adsorption, primarily driven by the formation of robust chemical bonds between the inhibitor molecules and the metal substrate. However, the proximity of this value to $-20\ kJmol^{-1}$ also hints at the

presence of physical interactions contributing to the adsorption process. This combination of chemical and physical interactions is commonly observed in real-world adsorption systems, where the adsorbate interacts both chemically and physically with the adsorbent surface. To summarize, at various temperatures (303 K, 313 K, 323 K, and 333 K), the standard Gibbs free energy changes for adsorption (ΔG^o_{ads} have been calculated to be approximately $-35.03\ kJmol^{-1}$, $-35.75\ kJmol^{-1}$, $-36.47\ kJmol^{-1}$, and $-37.19\ kJmol^{-1}$, respectively, all with units. These values suggest a coexistence of chemisorption and physisorption mechanisms, with chemisorption being the dominant driving force for adsorption on the metal surface.

4.3 Quantum Chemical Calculations

Quantum chemical calculations offer valuable insights into the behavior of the MPO inhibitor at the molecular level. Table 1 and Figure 6, displays the quantum chemical parameters and optimized molecular structure of MPO obtained through the B3LYP/6-311 G(d,p) approach. These calculations provide essential electronic and chemical properties crucial for understanding the inhibitor's role in corrosion inhibition in acidic environments [57,58].

Table 1. Quantum Chemical Properties of the Inhibitor Molecule.

Property	Value
EHOMO	-8.182 eV
ELUMO	21.986 eV
Energy Gap (Egap)	-13.804 eV
Hardness (η)	6.902 eV
Electronegativity (χ)	-15.084 eV
ΔN	≈ 1.598

4.3.1 EHOMO and ELUMO Analysis

The EHOMO (Highest Occupied Molecular Orbital) and ELUMO (Lowest Unoccupied Molecular Orbital) values provide crucial insights into the electron-donating and accepting capabilities of the MPO inhibitor. These properties play a fundamental role in understanding its effectiveness as a corrosion inhibitor in acidic environments. With an EHOMO value of -8.182 eV and an ELUMO value of 21.986 eV, there exists a substantial energy difference between these two orbitals. This energy gap underscores the

inhibitor's ability to participate efficiently in electron exchange processes. Specifically, the EHOMO represents the electron-donating capability (HOMO), while the ELUMO indicates its electron-accepting capacity (LUMO). These characteristics are paramount for the inhibitor's role in mitigating corrosion [59-61].
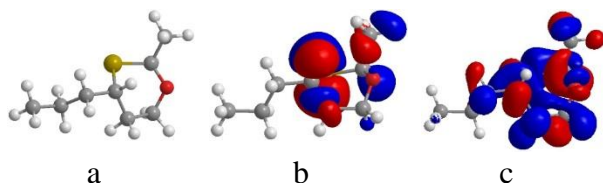
Fig. 6. a, Optimized structure, b, HOMO and c, LUMO Molecular Orbitals of MPO.

An examination of the HOMO of MPO, as depicted in Figure 6, highlights the electron-donating nature of the molecule. Notably, the sulfur and oxygen atoms within the inhibitor exhibit a strong propensity to transfer electrons to the metallic substrate. This behavior is a key attribute, as it enables the inhibitor to donate electrons effectively, thereby participating in the corrosion inhibition process [62]. Similarly, Figure 8 illustrates the LUMO shape of MPO, shedding light on its electron-accepting potential. The oxygen, sulfur, and carbon atoms featured in the LUMO positions are notably reactive, signifying their capacity to receive electrons from the surrounding environment. A low EHOMO value for MPO underscores its efficient electron-donating ability, while the ELUMO value indicates its readiness to accept electrons, suggesting a balanced electron exchange behavior. Overall, the EHOMO and ELUMO values, as well as the analysis of molecular orbitals, corroborate the inhibitor's suitability as a corrosion inhibitor. Its ability to both donate and accept electrons is fundamental for forming robust interactions with the metal surface, contributing to its corrosion inhibition effectiveness. These insights from quantum chemical calculations align seamlessly with experimental data, reinforcing the inhibitor's potential in real-world applications.

4.3.2 Energy Gap (Egap) Calculation:

The energy gap, calculated as the difference between ELUMO and EHOMO, is approximately -13.804 eV. This small energy gap indicates that the inhibitor can both donate and accept electrons readily. Its versatile electron behavior is advantageous for forming strong bonds and

interactions with the metal surface, enhancing its reactivity and adsorption capacity—a fundamental requirement for efficient corrosion inhibition [62,63]. Analysis of the quantum chemical parameters reveals that the inhibitor serves as an effective corrosion inhibitor. The low ΔE and η values, along with high σ and ΔN values, further substantiate its efficacy. These findings align remarkably well with the experimental data, supporting the theory that the metallic substrate engages in electron sharing (back-donation) with the inhibitor. In summary, the quantum chemical calculations provide valuable insights into the inhibitor's electronic and chemical attributes, reinforcing its potential as an efficient corrosion inhibitor in acidic environments. These findings bridge the gap between theory and experimental observations, enhancing our understanding of the corrosion inhibition mechanism.

4.3.3 Chemical Reactivity Parameters

Hardness (η): With a hardness value of 6.902 eV, the inhibitor exhibits stability in terms of electron addition or removal. This stability is a favorable characteristic as it contributes to the inhibitor's ability to maintain a protective film on the metal surface, even in corrosive environments. The robustness of this film is essential for long-term corrosion inhibition [63,64]. Electronegativity (χ): The negative electronegativity value of -15.084 eV indicates that the inhibitor has an inherent tendency to attract electrons. This electronegativity promotes its ability to form coordination bonds with metal atoms on the surface of the mild steel. These interactions are fundamental for adsorption and subsequent corrosion inhibition. Fractional Number of Transferred Electrons (ΔN): The calculated ΔN value, approximately 1.598, quantifies the transfer of electrons during chemical reactions involving the inhibitor. A positive ΔN indicates that the inhibitor is primarily an electron donor, which aligns with its observed role as a corrosion inhibitor. This electron-donating capability contributes to its ability to neutralize corrosion processes by donating electrons to active sites on the metal surface. In summary, the computational results presented in Table 1 provide valuable insights into the electronic and chemical attributes of the inhibitor. These calculations support the experimental findings and contribute to our understanding of the inhibitor's mechanism of action and its effectiveness as a corrosion inhibitor in acidic environments.

4.3.4 Correlation Between Computational and Experimental Results

The computational results presented here align with the experimental findings, such as the corrosion inhibition efficiency observed through weight loss tests. The small Egap, high hardness, and negative electronegativity collectively indicate that the inhibitor is proficient in adsorbing onto the metal surface and participating in corrosion inhibition processes. The positive ΔN confirms its role as an electron donor, further supporting its effectiveness in reducing corrosion rates. In summary, the computational results based on EHOMO, ELUMO, and chemical reactivity parameters offer valuable insights into the inhibitor's electronic and chemical attributes. These properties complement the experimental data and provide a comprehensive understanding of the inhibitor's mechanism of action and its potential as an efficient corrosion inhibitor in acidic environments [57-64].

4.4 Mechanism of Inhibition and Suggested Inhibition Mechanism

The understanding of the inhibition mechanism is pivotal for unraveling the effectiveness of corrosion inhibitors. In the case of the tested inhibitor, Figure 4 provides valuable insights into the effect of immersion time for mild steel in a 1 M HCl solution. The observed trends, coupled with quantum chemical calculations, allow us to propose a plausible inhibition mechanism [65].

4.4.1 Chemisorption: Coordination Bonds

One of the primary mechanisms at play in the inhibition process is chemisorption, wherein strong chemical bonds are formed between the inhibitor and the metal surface. In the context of our inhibitor, this mechanism involves the coordination bonds between the iron d-orbitals on the mild steel surface and the heteroatoms sulfur and oxygen present in the inhibitor molecule. This coordination leads to the formation of robust chemical bonds, which significantly contribute to the inhibition process [66].

4.4.2 Physisorption: Van der Waals Forces

In addition to chemisorption, physisorption also plays a significant role in the inhibition mechanism. Physisorption is characterized by weaker physical interactions, primarily driven by van der Waals forces, between the inhibitor and the metal surface. These interactions, while not as strong as chemical bonds, are still vital in enhancing the inhibitor's adsorption onto the metal substrate [67].

4.4.3 Suggested Inhibition Mechanism

The observed inhibitory behavior of the tested inhibitor is likely a result of the synergistic interplay between chemisorption and physisorption mechanisms. The coordination bonds formed through chemisorption, particularly between the iron d-orbitals and the inhibitor's sulfur and oxygen heteroatoms, are responsible for the stability and irreversible nature of the adsorption process. These chemical bonds effectively hinder the corrosion process by blocking active sites on the metal surface. Simultaneously, physisorption, driven by van der Waals forces, contributes to the inhibitor's adsorption capacity. While these interactions may be weaker, they are instrumental in facilitating the adsorption of inhibitor molecules onto the metal surface [65-67]. In conclusion, the inhibition mechanism of the tested inhibitor is multifaceted, involving both chemisorption and physisorption. The coordination bonds formed through chemisorption provide stability and irreversibility to the adsorption process, while van der Waals forces in physisorption enhance the adsorption capacity. This dual mechanism underscores the inhibitor's efficacy in protecting mild steel from corrosive attack in acidic environments. Further studies and investigations can provide deeper insights into the intricate details of this inhibition mechanism, paving the way for improved corrosion inhibition strategies.

4.5 Comparison with Recent Corrosion Inhibitors

Comparison of the inhibition efficiency of methyl MPO with recently reported corrosion inhibitors. In this section, we evaluate the performance of MPO as a corrosion inhibitor by comparing it with other inhibitors reported in similar corrosive environments, specifically focusing on the context of 1 M HCl. This comparative analysis provides valuable insights into the effectiveness of MPO and its suitability for corrosion protection under these conditions.

4.5.1 MPO

Our tested inhibitor, MPO, has exhibited a significant inhibitory efficiency. It achieved an impressive inhibition efficiency of 87.6% at an optimized concentration of 5 mM when tested at 303 K. This result underscores the remarkable potential of MPO as a corrosion inhibitor in 1 M HCl.

4.5.2 DBPBT: 1,1′-Dibenzyl-5-Phenyl-1H,1′H-4,4′-Bi(1,2,3-Triazole)

One notable inhibitor, 1,1′-dibenzyl-5-phenyl-1H,1′H-4,4′-bi(1,2,3-triazole) (DBPBT), has demonstrated remarkable inhibitory efficiency. DBPBT exhibited an inhibitory efficiency (IE%) of 96.32% at 100 ppm when tested at 302 K. However, it's essential to consider the temperature sensitivity of DBPBT, as its efficiency dropped to 87.91% at a higher temperature of 332 K. This observation emphasizes the significance of assessing corrosion inhibitors under varying environmental conditions, as temperature can significantly impact their performance [67].

4.5.3 PCBPE: 1H-Pyrazole-3,5-Dicarboxylic Acid 5-Benzyl Ester 3-Phenyl Ester

Another corrosion inhibitor, 1H-pyrazole-3,5-dicarboxylic acid 5-benzyl ester 3-phenyl ester (PCBPE), has shown promise as a protector against steel deterioration in 1 M HCl. At a concentration of 100 ppm, PCBPE achieved an inhibitory efficiency of up to 90.02% in this corrosive medium. Interestingly, beyond 100 ppm concentration of PCBPE, there was no remarkable variation in its inhibitory performance. This observation suggests the presence of an optimal concentration range for corrosion inhibition with PCBPE [68].

4.5.4 APCE: 5-Acetyl-2H-Pyrazole-3-Carboxylic Acid Ethyl Ester

Furthermore, we investigated 5-Acetyl-2H-pyrazole-3-carboxylic acid ethyl ester (APCE) as an anticorrosive agent for mild steel exposed to 1 M HCl at various temperatures. APCE exhibited a corrosion inhibition efficiency of 90.75% at a concentration of 100 ppm. This finding indicates that APCE possesses substantial inhibitory properties, making it an effective inhibitor in this aggressive acid solution [69].

In addition to the previously mentioned inhibitors, several other corrosion inhibitors have been investigated in recent studies, including 4-Aminoantipyrine derivatives [70], Schiff Base-Quinazoline [71], 1-amino-2-mercapto-5-(4-(pyrrol-1-yl)phenyl)-1,3,4-triazole [72], 3-Nitrobenzaldehyde-4-phenylthiosemicarbazone [73], and N-MEH [74]. However, a comparative analysis reveals that our corrosion inhibitor, MPO, offers several distinct advantages. Firstly, one notable advantage of our inhibitor is its cost-effectiveness and ease of synthesis. MPO can be synthesized using straightforward and economical methods, making it an attractive choice for industrial applications where cost considerations are paramount. Furthermore, our inhibitor exhibits a unique response to temperature variations. Unlike some of the aforementioned inhibitors that experienced a reduction in inhibition efficiency at higher temperatures, MPO demonstrated an increase in inhibition efficiency with rising temperatures. This temperature-dependent behavior enhances its versatility, allowing for effective corrosion protection even in elevated-temperature environments [75,76]. Another advantageous characteristic of our inhibitor is its response to immersion time. As demonstrated in our study, the inhibition efficiency of MPO increased with longer immersion times. This property is particularly valuable for applications where extended exposure to corrosive conditions is expected. In summary, while various inhibitors have been explored in recent research, MPO stands out as a promising candidate due to its cost-effectiveness, ease of synthesis, and its unique ability to enhance inhibition efficiency with increasing temperature and immersion time. These distinctive features make it a valuable contender for industrial corrosion protection strategies across a range of challenging environments." In this comparison, it is crucial to emphasize that all these inhibitors were evaluated within the same corrosive medium, 1 M HCl. This common test environment allows for a direct assessment of their relative performances. However, it is evident that each inhibitor exhibits unique characteristics and performance variations under different conditions, including temperature and concentration. The choice of a corrosion inhibitor should be tailored to the specific environmental parameters and corrosion protection requirements of the industrial application. Factors such as temperature sensitivity, optimal concentration range, and

inhibitory efficiency under varying conditions must be considered. Further investigations and comparative studies are essential for refining the selection of corrosion inhibitors to ensure optimal performance in diverse scenarios. These findings contribute to the ongoing development of effective corrosion protection strategies in various industrial contexts.

5. CONCLUSION

In this comprehensive study, we investigated the corrosion inhibition potential of MPO for mild steel in a 1 M HCl solution. The research was conducted using weight loss techniques, quantum chemical calculations, and adsorption isotherm models. The following key conclusions can be drawn from our findings:

5.1 Corrosion Inhibition Efficacy

The inhibitor demonstrated remarkable corrosion inhibition capabilities, with its effectiveness increasing as the inhibitor concentration rose. At a concentration of 0.5 mM, the inhibitor exhibited an impressive inhibitory efficiency of 87.6% during a 5-hour exposure period at 303 K. This effect can be attributed to the inhibitor's thioxane ring, which enhances electron density at active sites, facilitating interactions with iron, oxygen, and sulfide atoms.

5.2 Temperature Dependency

The inhibitor's inhibition efficiency was found to be temperature-dependent, with higher temperatures leading to enhanced inhibition. This temperature effect was explained by both chemisorption and physisorption mechanisms, where the inhibitor forms bonds with the iron d-orbitals on the mild steel surface.

5.3 Immersion Time Influence

Extended immersion periods resulted in more substantial corrosion reduction, with the inhibitor displaying the most significant inhibitory efficacy during immersion periods spanning from 10 to 24 hours. The adsorption density of the inhibitor increased during longer exposure, facilitating both physisorption and chemisorption processes.

5.4 Quantum Chemical Calculations

Quantum chemical calculations provided crucial insights into the electronic and chemical properties of the inhibitor. The EHOMO and ELUMO values demonstrated the inhibitor's electron-donating and electron-accepting capabilities, essential for its role as a corrosion inhibitor. The calculated energy gap (Egap) indicated the inhibitor's versatility in electron donation and acceptance, enhancing its reactivity and adsorption capacity.

5.5 Adsorption Isotherms

Adsorption isotherms revealed that the Langmuir model best described the adsorption process, suggesting a monolayer adsorption mechanism with a fixed maximum capacity. Additionally, the Temkin and Freundlich isotherms hinted at the presence of heat-driven and heterogeneous adsorption processes, respectively.

5.6 Inhibition Mechanism

The inhibition mechanism was proposed to involve both chemisorption and physisorption. Coordination bonds formed through chemisorption provided stability, while van der Waals forces in physisorption enhanced adsorption capacity.

In conclusion, the tested inhibitor, MPO, exhibited significant promise as a corrosion inhibitor for mild steel in acidic environments. Its inhibition efficiency, temperature dependence, and immersion time influence, supported by quantum chemical calculations and adsorption isotherm models, underscore its potential for practical applications in corrosion protection strategies. Further research in this direction holds promise for optimizing and developing more effective corrosion inhibition approaches, contributing to the mitigation of corrosion-related challenges in various industrial sectors.

REFERENCES

[1] S. Junaedi, A. A. H. Kadhum, A. Al-Amiery, A. B. Mohamad, M. S. Takriff, "Synthesis and characterization of novel corrosion inhibitor derived from oleic acid: 2-Amino-5-Oleyl 1,3,4-Thiadiazol (AOT)," *Int J Electrochem Sci*, vol. 7, pp. 3543-3554, 2012.

[2] A. Alobaidy, A. Kadhum, S. Al-Baghdadi, A. Al-Amiery, A. Kadhum, E. Yousif, A. B. Mohamad, "Eco-friendly corrosion inhibitor: experimental studies on the corrosion inhibition performance of creatinine for mild steel in HCl complemented with quantum chemical calculations," *Int J Electrochem Sci*, vol. 10, pp. 3961-3972, 2015.

[3] S. Al-Bghdadi, M. Hanoon, J. Odah, L. Shaker, A. Al-Amiery, "Benzylidene as Efficient Corrosion Inhibition of Mild Steel in Acidic Solution," *Proceedings*, vol. 41, p. 27, 2019.

[4] B. S. Mahdi, H. S. S. Aljibori, M. K. Abbass, W. K. Al-Azzawi, A. H. Kadhum, M. M. Hanoon, W. N. R. W. Isahak, A. A. Al-Amiery, H. Majdi, "Gravimetric analysis and quantum chemical assessment of 4-aminoantipyrine derivatives as corrosion inhibitors," *Int J Corros Scale Inhib*, vol. 11, no. 3, pp. 1191-1213, 2022.

[5] A. Alamiery, "Study of Corrosion Behavior of N´-(2-(2-oxomethylpyrrol-1-yl) ethyl) piperidine for Mild Steel in the Acid Environment," *Biointerface Res Appl Chem*, vol. 12, pp. 3638-3646, 2022.

[6] A. Alamiery, A. B. Mohamad, A. Kadhum, M. S. Takriff, "Comparative data on corrosion protection of mild steel in HCl using two new thiazoles," *Data Brief*, vol. 40, p. 107838, 2022.

[7] M. Mustafa, F. F. Sayyid, N. Betti, L. M. Shaker, M. M. Hanoon, A. A. Alamiery, A. A. H. Kadhum, M. S. Takriff, "Inhibition of mild steel corrosion in HCl environment by 1-amino-2-mercapto-5-(4-(pyrrol-1-yl)phenyl)-1,3,4-triazole," *S Afr J Chem Eng*, vol. 39, pp. 42-51, 2022.

[8] A. Alamiery, "Investigations on corrosion inhibitory effect of newly quinoline derivative on mild steel in HCl solution complemented with antibacterial studies," *Biointerface Res Appl Chem*, vol. 12, pp. 1561-1568, 2022.

[9] A. Alamiery, "Short report of mild steel corrosion in 0.5 M H2SO4 by 4-ethyl-1-(4-oxo4-phenylbutanoyl)thiosemicarbazide," *Tribologi*, vol. 30, pp. 90-99, 2021.

[10] A. Alamiery, W. N. R. W. Isahak, M. S. Takriff, "Inhibition of mild steel corrosion by 4-benzyl-1-(4-oxo-4-phenylbutanoyl)thiosemicarbazide: Gravimetrical, adsorption and theoretical studies," *Lubricants*, vol. 9, no. 9, p. 93, 2021.

[11] M. A. Dawood, Z. M. K. Alasady, M. S. Abdulazeez, D. S. Ahmed, G. M. Sulaiman, A. A. H. Kadhum, L. M. Shaker, A. A. Alamiery, "The corrosion inhibition effect of a pyridine derivative for low carbon steel in 1 M HCl medium: Complemented with antibacterial studies," *Int J Corros Scale Inhib*, vol. 10, pp. 1766-1782, 2021.

[12] A. Alamiery, W. N. R. W. Isahak, H. Aljibori, H. Al-Asadi, A. Kadhum, "Effect of the structure, immersion time and temperature on the corrosion inhibition of 4-pyrrol-1-yln-(2,5-dimethyl-pyrrol-1-yl)benzoylamine in 1.0 m HCl solution," *Int J Corros Scale Inhib*, vol. 10, pp. 700-713, 2021.

[13] A. Alamiery, E. Mahmoudi, T. Allami, "Corrosion inhibition of low-carbon steel in HCl environment using a Schiff base derived from pyrrole: gravimetric and computational studies," *Int. J. Corros. Scale Inhib.*, vol. 10, pp. 749–765, 2021.

[14] J. M. Eltmimi, A. Alamiery, A. J. Allami, R. M. Yusop, A. H. Kadhum, T. Allami, "Inhibitive effects of a novel efficient Schiff base on mild steel in HCl environment," *Int. J. Corros. Scale Inhib.*, vol. 10, pp. 634–648, 2021.

[15] A. Alamiery, L. M. Shaker, T. Allami, A. H. Kadhum, M. S. Takriff, "A study of acidic corrosion behavior of Furan-Derived Schiff base for mild steel in HCl environment: Experimental, and surface investigation," *Mater. Today: Proc.*, vol. 44, pp. 2337–2341, 2021.

[16] S. Al-Baghdadi, A. Al-Amiery, T. Gaaz, A. Kadhum, "Terephthalohydrazide and isophthalohydrazide as new corrosion inhibitors for mild steel in HCl: Experimental and theoretical approaches," *Koroze Ochr. Mater.*, vol. 65, pp. 12–22, 2021.

[17] M. M. Hanoon, A. M. Resen, L. M. Shaker, A. Kadhum, A. Al-Amiery, "Corrosion investigation of mild steel in aqueous HCl environment using n- (Naphthalen-1yl)-1-(4-pyridinyl)methanimine complemented with antibacterial studies," *Biointerface Res. Appl. Chem.*, vol. 11, pp. 9735–9743, 2021.

[18] A. K. Khudhair, A. M. Mustafa, M. M. Hanoon, A. Al-Amiery, L. M. Shaker, T. Gazz, et al., "Experimental and Theoretical Investigation on the Corrosion Inhibitor Potential of N-MEH for Mild Steel in HCl," *Prog. Color, Color. Coat.*, vol. 15, pp. 111–122, 2022.

[19] D. S. Zinad, R. D. Salim, N. Betti, L. M. Shaker, A. A. Al-Amiery, "Comparative Investigations of the Corrosion Inhibition Efficiency of a 1-phenyl-2-(1-phenylethylidene)hydrazine and its Analog Against Mild Steel Corrosion in HCl Solution," *Prog. Color, Color. Coat.*, vol. 15, pp. 53–63, 2022.

[20] M. Damej, A. Molhi, K. Tassaoui, B. El Ibrahimi, Z. Akounach, A. Ait Addi, S. El hajjaji, M. Benmessaoud, "Experimental and Theoretical Study to Understand the Adsorption Process of p-Anisidine and 4-Nitroaniline for the Dissolution of C38 Carbon Steel in 1M HCl," *Chemistry Select Volume 7, Issue 2*, Jan 12, 2022.

[21] F. Bouhlal et al., "Combination effect of hydro-alcoholic extract of spent coffee grounds (HECG) and potassium Iodide (KI) on the C38 steel corrosion inhibition in 1M HCl medium: Experimental design by response surface methodology," *Chemical Data Collections*, vol. 29, p. 100499, 2020.

[22] Y. El Hamdouni et al., "Use of Omeprazole as Inhibitor for C38 Steel Corrosion in 1.0 M H3PO4 Medium," *Journal of Failure Analysis and Prevention*, vol. 20, no. 2, pp. 563–571, 2020.

[23] Z. Akounach et al., "Inhibition of mild steel corrosion in 1.0 M HCl by water, hexane and ethanol extracts of pimpinella anisum plant," *Analytical and Bioanalytical Electrochemistry*, vol. 10, no. 11, pp. 1506–1524, 2018.

[24] M. Abouchane et al., "Exploratory Experiments Supported by Modeling Approaches for TGEEA New Epoxy Resin as a Contemporary Anti-corrosion Material for C38 Steel in 1.0 M HCl," *Journal of Failure Analysis and Prevention*, pp. 1-17.

[25] M. Manssouri et al., "Aqueous extracts of Aaronsohnia pubescens subsp. pubescens aerial parts as Green Corrosion Inhibitor for Mild Steel in HCl solution," *Journal of the Turkish Chemical Society Section A: Chemistry*, vol. 8, no. 3, pp. 953-968.

[26] N. B. Seddik et al., "Highlighting performances of lanthanum-intercalated stevensite and the commercially available triphosphate aluminium (TPA) as anticorrosive pigments for brass in 3 % NaCl solution: Electrochemical and morphological study," *Progress in Organic Coatings*, vol. 147, p. 105837.

[27] N. B. Seddik et al., "Calcite, the main corrosion inhibitor contained in the raw clay (Rhassoul) of brass in 3% NaCl medium," *Mediterranean Journal of Chemistry*, vol. 9, no. 3, pp. 236-248.

[28] R. D. Salim et al., "2-(2,4-Dimethoxybenzylidene)-N-Phenylhydrazinecarbothioamide as an Efficient Corrosion Inhibitor for Mild Steel in Acidic Environment," *Prog. Color, Color. Coat.*, vol. 15, pp. 45–52, 2021.

[29] D. M. Jamil et al., "Carbethoxythiazole corrosion inhibitor: as an experimentally model and DFT theory," *J Eng Appl Sci.*, vol. 13, pp. 3952-3959, 2018.

[30] A. Alkadir Aziz et al., "Insights into Corrosion Inhibition Behavior of a 5-Mercapto-1, 2, 4-triazole Derivative for Mild Steel in HCl Solution: Experimental and DFT Studies," *Lubricants*, vol. 9, no. 9, p. 122, 2021.

[31] A. Alamiery, "Corrosion inhibition effect of 2-N-phenylamino-5-(3-phenyl-3-oxo-1-propyl)-1,3,4-oxadiazole on mild steel in 1 M HCl medium: Insight from gravimetric and DFT investigations," *Mater Sci Energy Technol.*, vol. 4, pp. 398-406, 2021.

[32] S. Al-Baghdadi et al., "Experimental studies on corrosion inhibition performance of acetylthiophene thiosemicarbazone for mild steel in HCl complemented with DFT investigation," *Int. J. Low-Carbon Technol.*, vol. 16, pp. 181–188, 2021.

[33] M. S. Abdulazeez et al., "Corrosion inhibition of low carbon steel in HCl medium using a thiadiazole derivative: weight loss, DFT studies and antibacterial studies," *Int. J. Corros. Scale Inhib.*, vol. 10, pp. 1812–1828, 2021.

[34] A. Mustafa et al., "Inhibition Evaluation of 5-(4-(1H-pyrrol-1-yl)phenyl)-2-mercapto-1,3,4-oxadiazole for the Corrosion of Mild Steel in an Acid environment: Thermodynamic and DFT Aspects," *Tribologia.*, vol. 38, pp. 39–47, 2021.

[35] Y. M. Abdulsahib et al., "Experimental and theoretical investigations on the inhibition efficiency of N-(2,4-dihydroxytolueneylidene)-4-methylpyridin-2-amine for the corrosion of mild steel in HCl," *Int. J. Corros. Scale Inhib.*, vol. 10, pp. 885–899, 2021.

[36] A. A. Al-Amiery, "Anti-corrosion performance of 2-isonicotinoyl-n-phenylhydrazinecarbothioamide for mild steel HCl solution: Insights from experimental measurements and quantum chemical calculations," *Surf. Rev. Lett.*, vol. 28, p. 2050058, 2021.

[37] W. K. Al-Azzawi et al., "Adsorption and theoretical investigations of a Schiff base for corrosion inhibition of mild steel in an acidic environment," *Int J Corros Scale Inhib.*, vol. 11, no. 3, pp. 1063-1082, 2022.

[38] H. S. Aljibori et al., "The use of a Schiff base derivative to inhibit mild steel corrosion in 1 M HCl solution: a comparison of practical and theoretical findings," *Int J Corros Scale Inhib.*, vol. 11, no. 4, pp. 1435-1455, 2022.

[39] A. A. Alamiery, "Anticorrosion effect of thiosemicarbazide derivative on mild steel in 1 M HCl and 0.5 M sulfuric Acid: Gravimetrical and theoretical studies," *Mater Sci Energy Technol.*, vol. 4, pp. 263-273, 2021.

[40] ASTM International, "Standard Practice for Preparing, Cleaning, and Evaluating Corrosion Test," ASTM International, 2011.

[41] NACE International, "Laboratory Corrosion Testing of Metals in Static Chemical Cleaning Solutions at Temperatures below 93°C (200°F), TM0193-2016-SG, 2000."

[42] M. J. Frisch et al., *Gaussian 03, Revision B. 05*, Gaussian, Inc., Wallingford, CT, 2004.

[43] T. Koopmans, "Ordering of wave functions and eigen-energies to the individual electrons of an atom," *Physica*, 1934, 1:104–113.

[44] A. A. Al-Amiery et al., "Exploration of furan derivative for application as corrosion inhibitor for mild steel in HCl solution: Effect of immersion time and temperature on efficiency," *Mater. Today: Proc.*, 2021, 42:2968–2973.

[45] A. M. Resen et al., "Exploration of 8-piperazine-1-ylmethylumbelliferone for application as a corrosion inhibitor for mild steel in HCl solution," *Int. J. Corros. Scale Inhib.*, 2021, 10:368–387.

[46] F. G. Hashim et al., "Inhibition effect of hydrazine-derived coumarin on a mild steel surface in HCl," *Tribologia*, 2020, 37:45–53.

[47] A. Z. Salman et al., "Selected BISThiadiazole: Synthesis and Corrosion Inhibition Studies on Mild Steel in HCL Environment," *Surf. Rev. Lett.*, 2020, 27:2050014.

[48] S. Junaedi et al., "Inhibition effects of a synthesized novel 4-aminoantipyrine derivative on the corrosion of mild steel in HCl solution together with quantum chemical studies," *Int. J. Mol. Sci.*, 2013, 14:11915–11928.

[49] A. Alamiery et al., "Effect of the structure, immersion time and temperature on the corrosion inhibition of 4-pyrrol-1-yl-n-(2,5-dimethyl-pyrrol-1-yl)benzoylamine in 1.0 M HCL solution," *Int. J. Corros. Scale Inhib.*, 2021, 10:700–713.

[50] W. K. Al-Azzawi et al., "Evaluation of corrosion inhibition characteristics of an N-propionanilide derivative for mild steel in 1 M HCl: Gravimetrical and computational studies," *Int. J. Corros. Scale Inhib.*, 2022, 11:1100–1114.

[51] A. A. Al-Amiery et al., "Corrosion Inhibitors: Natural and Synthetic Organic Inhibitors," *Lubricants*, 2023, 11:174.

[52] A. A. Al-Amiery et al., "ODHI: A Promising Isatin-Based Corrosion Inhibitor for Mild Steel in HCl," *Journal of Molecular Structure*, 2023, 135829.

[53] A. A. Al-Amiery et al., "Exploring the Effectiveness of Isatin–Schiff Base as an Environmentally Friendly Corrosion Inhibitor for Mild Steel in HCl," *Lubricants*, 2023, 11:211.

[54] A. K. Al-Edan et al., "Palmitic acid-based amide as a corrosion inhibitor for mild steel in 1M HCl," *Heliyon*, 2023, 9:e08625.

[55] A. A. Al-Amiery, "Schiff's base performance in preventing corrosion on mild steel in acidic conditions," *Progress in Color, Colorants and Coatings*, 2023.

[56] A. A. Al-Amiery, "Investigation of the Corrosion Inhibition Properties of 4-Cyclohexyl-3-Thiosemicarbazide on Mild Steel in 1 M HCl Solution," *Prog. Color Colorants Coat.*, 16 (2023), 347-359.

[57] M. M. Hanoon et al., "Theoretical and Experimental Studies on the Corrosion Inhibition Potentials of 2-((6-Methyl-2-Ketoquinolin-3-yl)Methylene)Hydrazinecarbothioamide for Mild Steel in 1 M HCl," *Prog. Color, Color. Coat.*, 2021, 15:21–33.

[58] A. M. Resen et al., "Gravimetrical, theoretical, and surface morphological investigations of corrosion inhibition effect of 4-(benzoimidazole-2-yl)pyridine on mild steel in HCl," *Koroze Ochr. Mater.*, 2020, 64:122–130.

[59] S. Baghdadi et al., "Synthesis and corrosion inhibition application of NATN on mild steel surface in acidic media complemented with DFT studies," *Results Phys.*, 2018, 8:1178–1184.

[60] N. Betti et al., "Corrosion inhibition properties of Schiff base derivative against mild steel in HCl environment complemented with DFT investigations," *Scientific Reports*, 2023, 13:8979.

[61] A. Alamiery, "Case Study in a Conceptual DFT Investigation of New Corrosion Inhibitor," *Letters in Applied NanoBioScience*, 2021, 11:4007–4015.

[62] K. M. Raheef et al., "Gravimetric and Density Functional Theory Investigations on 4-Aminoantipyrin Schiff Base as an Inhibitor for Mild Steel in HCl Solution," *Progress in Color, Colorants and Coatings*, 2023, 16:255–269.

[63] N. Betti et al., "Synthesis and study of corrosion behavior of terephthalaldehyde-derived schiff base for low-carbon steel in HCl: experimental, morphological and theoretical investigation," *KOM–Corrosion and Material Protection Journal*, 2022, 66:103–112.

[64] A. A. Hussein et al., "Antibacterial Corrosion Inhibitor for the Protection of Mild Steel in 1 M HCl Solution," *Prog. Color Color. Coat.*, 2023, 16:59–70.

[65] A. A. Al-Amiery, "Effect of Temperature on the Corrosion Inhibition of 4-ethyl-1-(4-oxo-4-phenylbutanoyl)thiosemicarbazide on Mild Steel in HCl Solution," *Letters in Applied NanoBioScience*, 2022, 11:3502–3508.

[66] M. S. Carranza et al., "Electrochemical and quantum mechanical investigation of various small molecule organic compounds as corrosion inhibitors in mild steel," *Heliyon*, 2021, 7:e08625.

[67] N. Punitha et al., "Bis-1, 2, 3-triazole derivative as an efficient corrosion inhibitor for mild steel in hydrochloric acid environment: Insights from experimental and computational analysis," *Inorganic Chemistry Communications*, 2023, 153:110732.

[68] N. Punitha et al., "Corrosion mitigation performance of pyrazole derivative on mild steel in acidic media: Electrochemical and theoretical approach," *Chemical Data Collections*, 2022, 41:100936.

[69] N. Punitha et al., "Interactions and corrosion mitigation prospective of pyrazole derivative on mild steel in HCl environment," *Journal of the Indian Chemical Society*, 2022, 99:9, 100667.

[70] F. F. Sayyid et al., "Gravimetric Measurements and Theoretical Calculations of 4-Aminoantipyrine Derivatives as Corrosion Inhibitors for Mild Steel in Hydrochloric Acid Solution: Comparative Studies," *Corrosion Science and Technology*, 2023, 22:2, 73-89.

[71] F. F. Sayyid et al., "Corrosion Protection Effectiveness and Adsorption Performance of Schiff Base-Quinazoline on Mild Steel in HCl Environment," *Corrosion Science and Technology*, 2022, 21:2, 77-88.

[72] A. M. Mustafa et al., "Inhibition of mild steel corrosion in hydrochloric acid environment by 1-amino-2-mercapto-5-(4-(pyrrol-1-yl) phenyl)-1, 3, 4-triazole," *South African Journal of Chemical Engineering*, 2022, 39:1, 42-51.

[73] A. M. Mustafa et al., "3-Nitrobenzaldehyde-4-phenylthiosemicarbazone as Active Corrosion Inhibitor for Mild Steel in a Hydrochloric Acid Environment," *Progress in Color, Colorants and Coatings*, 2022, 15:4, 285-293.

[74] A. K. Khudhair et al., "Experimental and theoretical investigation on the corrosion inhibitor potential of N-MEH for mild steel in HCl," *Progress in Color, Colorants and Coatings*, 2022, 15:2, 111-122.

[75] A. Naseef Jasim et al., "Schiff's base performance in preventing corrosion on mild steel in acidic conditions," *Progress in Color, Colorants and Coatings*, 2023, 16:4, 319-329.

[76] A. A. Al-Amiery and W. K. Al-Azzawi, "Organic Synthesized Inhibitors for Corrosion Protection of Carbon Steel: A Comprehensive Review," *Journal of Bio-and Tribo-Corrosion*, 2023, 9:4, 74.